PHYSICAL REVIEW C **90**, 061602(R) (2014)

# Separable representation of proton-nucleus optical potentials

L. Hlophe,[1,*] V. Eremenko,[1,2] Ch. Elster,[1,†] F. M. Nunes,[3] G. Arbanas,[4] J. E. Escher,[5] and I. J. Thompson[5]
(TORUS Collaboration)
[1]*Institute of Nuclear and Particle Physics, and Department of Physics and Astronomy, Ohio University, Athens, Ohio 45701, USA*
[2]*D.V. Skobeltsyn Institute of Nuclear Physics, M.V. Lomonosov Moscow State University, Moscow, 119991, Russia*
[3]*National Superconducting Cyclotron Laboratory and Department of Physics and Astronomy, Michigan State University, East Lansing, Michigan 48824, USA*
[4]*Reactor and Nuclear Systems Division, Oak Ridge National Laboratory, Oak Ridge, Tennessee 37831, USA*
[5]*Lawrence Livermore National Laboratory L-414, Livermore, California 94551, USA*
(Received 14 September 2014; revised manuscript received 4 November 2014; published 9 December 2014)

Recently, a new approach for solving the three-body problem for (d,p) reactions in the Coulomb-distorted basis in momentum space was proposed. Important input quantities for such calculations are the scattering matrix elements for proton- (neutron-) nucleus scattering. We present a generalization of the the Ernst-Shakin-Thaler scheme in which a momentum space separable representation of proton-nucleus scattering matrix elements in the Coulomb basis can be calculated. The success of this method is demonstrated by comparing *S*-matrix elements and cross sections for proton scattering from $^{12}$C, $^{48}$Ca, and $^{208}$Pb with the corresponding coordinate space calculations.

DOI: 10.1103/PhysRevC.90.061602 PACS number(s): 24.10.Ht, 25.10.+s, 25.40.Cm

Deuteron induced nuclear reactions are attractive from an experimental as well as theoretical point of view to probe the structure of exotic nuclei. For example, carried out in inverse kinematics, (d,p) or (d,n) reactions prove useful for extracting neutron or proton capture rates on unstable nuclei of astrophysical relevance (see, e.g., [1]). From a theoretical perspective (d,p) reactions are attractive because the scattering problem can be viewed as an effective three-body problem [2]. One of the most challenging aspects of solving the three-body problem for nuclear reactions is the repulsive Coulomb interaction between the nucleus and the proton. While for very light nuclei, exact calculations of (d,p) reactions based on momentum-space Faddeev equations in the Alt-Grassberger-Sandhas (AGS) [3] formulation can be carried out [4], this is not the case for heavier nuclei with higher charges. The reason for this shortcoming stems from the implementation of the Faddeev-AGS equations, which relies on a screening and renormalization procedure [5,6], which leads to increasing technical difficulties in computing (d,p) reactions with heavier nuclei [7].

To avoid a screening procedure Ref. [8] derived a three-body theory for (d,p) reactions such that the Faddeev-AGS equations are cast in a momentum-space Coulomb-distorted partial-wave representation, instead of the plane-wave basis. Thus all operators, specifically the interactions in the two-body subsystems must be evaluated in the Coulomb basis, which is a nontrivial task (carried out recently for the neutron-nucleus interaction; see Ref. [9]). The formulation of Ref. [8] requires the interactions in the subsystems to be of separable form. Proton-proton ($pp$) scattering based on separable interactions was considered some time ago in [10] and [11,12]. Therein the $pp$ interaction was represented in terms of analytic functions, and the parameters in the two lowest partial waves were adjusted to describe the experimentally extracted $pp$ phase shifts. While such an approach is viable in the $pp$ system, it is not very practical when heavy nuclei are considered because here many more partial waves are affected by the Coulomb force. Separable forms for nucleon-nucleus interactions were considered only as rank-1 Yamaguchi functions [13,14], and were intended to represent the nuclear forces up to a few MeV.

In Ref. [15] we derived a separable representation of phenomenological neutron-nucleus optical potentials based on Woods-Saxon forms, using a generalization of the Ernst, Shakin, and Thaler (EST) scheme for non-Hermitian interactions. In this work we derive a momentum-space separable representation of proton-nucleus optical potentials in the Coulomb basis.

The derivations in the original EST work laid out in [16] set up the scattering problem in a complete plane-wave basis, whereas in this work we need to use a complete Coulomb basis. Consequently, when working in momentum space, we require that a solution of the momentum space scattering equation in the Coulomb basis exists. We solve the momentum space Lippmann-Schwinger (LS) equation in the Coulomb basis, following the method introduced in Ref. [17] and successfully applied in proton-nucleus scattering calculations with microscopic optical potentials in Ref. [18].

First, we sketch the important steps needed to derive a separable representation of a phenomenological global optical potential in the momentum-space Coulomb basis for proton-nucleus scattering. Our numerical calculations of *S*-matrix elements and cross sections for proton elastic scattering from $^{12}$C, $^{48}$Ca, and $^{208}$Pb at selected laboratory kinetic energies are then discussed along with the behavior of the form factors as a function of the external momentum.

*lh421709@ohio.edu
†elster@ohio.edu

 

The scattering between a proton and a nucleus is governed by a potential,

$$w = v^C + u^s, \tag{1}$$

where $v^C$ is the repulsive Coulomb potential and $u^s$ an arbitrary short-range potential. In general $u^s$ consists of a proton-nucleus optical potential $u^N$ describing the nuclear interactions, and a short-ranged Coulomb potential $v^{cd} - v^C$, traditionally parametrized as the potential of a charged sphere with radius $R_0$ of which the point Coulomb force is subtracted [19],

$$(v^{cd} - v^C)(r) = \alpha Z_1 Z_2 \left[\frac{1}{2R_0}\left(3 - \frac{r^2}{R_0^2}\right) - \frac{1}{r}\right], \tag{2}$$

with $Z_1$ and $Z_2$ being the atomic numbers of the particles, and $\alpha$ the Coulomb coupling constant. Because the scattering problem governed by the Coulomb force has an analytic solution with scattering wave functions that form a complete basis, the scattering amplitude for elastic scattering between a proton and a spin zero nucleus is obtained as the sum of the Rutherford amplitude $f^C(E_{p_0},\theta)$ and the Coulomb-distorted nuclear amplitude,

$$M^{CN}(E_{p_0},\theta) = f^{CN}(E_{p_0},\theta) + \hat{\sigma}\cdot\hat{\mathbf{n}}\, g^{CN}(E_{p_0},\theta), \tag{3}$$

with

$$\begin{aligned} f^{CN}(E_{p_0},\theta) = &-\pi\mu \sum_{l=0}^{\infty} e^{2i\sigma_l(E_{p_0})} P_l(\cos\theta) \\ &\times \left[(l+1)\langle p_0|\tau_{l+}^{CN}(E_{p_0})|p_0\rangle \right. \\ &\left. + l\langle p_0|\tau_{l-}^{CN}(E_{p_0})|p_0\rangle\right], \end{aligned} \tag{4}$$

$$\begin{aligned} g^{CN}(E_{p_0},\theta) = &-\pi\mu \sum_{l=0}^{\infty} e^{2i\sigma_l(E_{p_0})} P_l^1(\cos\theta) \\ &\times\left[\langle p_0|\tau_{l+}^{CN}(E_{p_0})|p_0\rangle - \langle p_0|\tau_{l-}^{CN}(E_{p_0})|p_0\rangle\right]. \end{aligned} \tag{5}$$

Here $E_{p_0} = p_0^2/2\mu$ is the center-of-mass (c.m.) scattering energy which defines the on-shell momentum $p_0$, $\sigma_l = \arg\Gamma(1+l+i\eta)$ is the Coulomb phase shift, and the Sommerfeld parameter is given by $\eta = \alpha Z_1 Z_2 \mu/p$. The unit vector $\hat{\mathbf{n}}$ is perpendicular to the scattering plane and $\hat{\sigma}/2$ is the spin operator. The subscripts "+" and "−" correspond to a total angular momentum of $j = l + 1/2$ and $j = l - 1/2$, respectively. Suppressing the total angular momentum indices for simplicity, the Coulomb-distorted nuclear $t$-matrix element is given by $\langle p_0|\tau_l^{CN}(E_{p_0})|p_0\rangle$, which is the solution of an LS-type equation,

$$\begin{aligned} \langle p|\tau_l^{CN}(E_{p_0})|p_0\rangle = &\langle p|u_l^s|p_0\rangle + \int p'^2 dp' \langle p|u_l^s|p'\rangle \\ &\times\langle p'|g_c(E_{p_0}+i\varepsilon)|p'\rangle\langle p'|\tau_l^{CN}(E_{p_0})|p_0\rangle. \end{aligned} \tag{6}$$

Here $g_c(E_{p_0}+i\varepsilon) = (E_{p_0}+i\varepsilon - H_0 - v^C)^{-1}$ is the Coulomb Green's function, and $H_0$ the free Hamiltonian. The Coulomb-distorted nuclear $t$-matrix element $\langle p|\tau_l^{CN}(E_{p_0})|p_0\rangle$ is related to the proton-nucleus $t$ matrix $\langle p|t_l(E_{p_0})|p_0\rangle$ by the familiar two-potential formula,

$$\langle p|t_l(E_{p_0})|p_0\rangle = \langle p|t_l^C(E_{p_0})|p_0\rangle + e^{2i\sigma_l(E_{p_0})}\langle p|\tau_l^{CN}(E_{p_0})|p_0\rangle, \tag{7}$$

where $\langle p|t_l^C(E_{p_0})|p_0\rangle$ is the point Coulomb $t$ matrix.

When the integral equation in Eq. (6) is solved in the basis of Coulomb eigenfunctions, $g_c$ acquires the form of a free Green's function and the difficulty of solving it is shifted to evaluating the potential matrix elements in this basis.

For deriving a separable representation of the Coulomb-distorted proton-nucleus $t$-matrix element, we generalize the approach suggested by Ernst, Shakin, and Thaler [16], to the charged particle case. The basic idea behind the EST construction of a separable representation of a given potential is that the wave functions calculated with this potential and the corresponding separable potential agree at given fixed scattering energies $E_i$, the EST support points. The formal derivations of [16] use the plane-wave basis, which is standard for scattering involving short-range potentials. However, the EST scheme does not depend on the basis and can equally well be carried out in the basis of Coulomb scattering wave functions. To generalize the EST approach to charged-particle scattering, one needs to be able to obtain the scattering wave functions or half-shell $t$ matrices from a given potential in the Coulomb basis.

To obtain the Coulomb-distorted short-range half-shell $t$-matrix element needed in Eq. (7), we solve Eq. (6) in the Coulomb basis as suggested in Ref. [17], and note that in this case the Coulomb Green's function behaves like a free Green's function. Taking $|\Phi_{l,p}^c\rangle$ to represent the partial-wave Coulomb eigenstate Eq. (6) reads

$$\begin{aligned} &\langle\Phi_{l,p}^c|\tau_l^{CN}(E_{p_0})|\Phi_{l,p_0}^c\rangle \\ &\quad= \langle\Phi_{l,p}^c|u_l^s|\Phi_{l,p_0}^c\rangle + \int_0^\infty \langle\Phi_{l,p}^c|u_l^s|\Phi_{l,p'}^c\rangle \\ &\qquad\times\frac{p'^2dp'}{E_{p_0} - E_{p'} + i\varepsilon}\langle\Phi_{l,p'}^c|\tau_l^{CN}(E_{p_0})|\Phi_{l,p_0}^c\rangle \\ &\quad\equiv \langle p|\tau_l^{CN}(E_{p_0})|p_0\rangle, \end{aligned} \tag{8}$$

defining the Coulomb-distorted short-range half-shell $t$ matrix. The essential ingredient is the driving term of Eq. (8). To obtain it we follow Ref. [17] and insert a complete set of position space eigenfunctions,

$$\begin{aligned} &\langle\Phi_{l,p'}^c|u_l^s|\Phi_{l,p}^c\rangle \\ &\quad= \frac{2}{\pi}\int_0^\infty \langle\Phi_{l,p'}^c|r'\rangle\, r'^2dr'\, \langle r'|u_l^s|r\rangle\, r^2dr\, \langle r|\Phi_{l,p}^c\rangle \\ &\quad= \frac{2}{\pi p' p}\int_0^\infty rr'drdr'\, F_l(\eta',p'r')\, \langle r'|u_l^s|r\rangle\, F_l(\eta,pr), \end{aligned} \tag{9}$$

where the coordinate-space partial-wave Coulomb functions are given as

$$\langle r|\Phi_{l,p}^c\rangle \equiv \Phi_{l,p}^c(r) \equiv \frac{F_l(\eta,\, pr)}{pr}. \tag{10}$$

For our application we consider phenomenological optical potentials of the Woods-Saxon form which are local in coordinate space. Thus the momentum-space potential matrix elements simplify to

$$\langle \Phi^c_{l,p'} | u^s_l | \Phi^c_{l,p} \rangle = \frac{2}{\pi p' p} \int_0^\infty dr\ F_l(\eta', p'r) u^s_l(r) F_l(\eta, pr). \tag{11}$$

We compute these matrix elements for the short-range piece of the CH89 phenomenological global optical potential [19], consisting of a nuclear and a short-range Coulomb potential, as given in Eq. (2). The integral can be carried out with standard methods because $u^s_l(r)$ is short ranged and the coordinate space Coulomb wave functions are well defined. The accuracy of this integral can be tested by replacing the Coulomb functions with spherical Bessel functions and comparing the resulting matrix elements to a partial-wave decomposition of the semianalytic Fourier transform in Ref. [15]. For a finite grid, a maximum radial value of 14 fm and 300 grid points is sufficient to obtain matrix elements with a precision of six significant figures.

Extending the EST separable representation to the Coulomb basis involves replacing the neutron-nucleus half-shell $t$ matrix in Eqs. (14)–(16) of Ref. [15] by Coulomb scattering states $|f^c_{l,p}\rangle$, which defines the Coulomb-distorted separable nuclear $t$ matrix,

$$\tau^{CN}_l(E_{p_0}) = \sum_{i,j} u^s_l \big| f^c_{l,k_{E_i}} \big\rangle\ \tau^c_{ij}(E_{p_0})\ \big\langle f^{c,*}_{l,k_{E_j}} \big| u^s_l, \tag{12}$$

with $\tau^c_{ij}(E_{p_0})$ being constrained by

$$\begin{aligned} \sum_i \big\langle f^{c*}_{l,k_{E_n}} \big| u^s_l - u^s_l g_c(E_{p_0}) u^s_l \big| f^c_{l,k_{E_i}} \big\rangle \tau^c_{ij}(E) &= \delta_{nj}, \\ \sum_j \tau^{CN}_{ij}(E_{p_0}) \big\langle f^{c*}_{l,k_{E_j}} \big| u^s_l - u^s_l g_c(E_{p_0}) u^s_l \big| f^c_{l,k_{E_k}} \big\rangle &= \delta_{ik}. \end{aligned} \tag{13}$$

Here $|f^c_{l,k_{E_i}}\rangle$ and $|f^{c,*}_{l,k_{E_i}}\rangle$ are the regular radial Coulomb scattering wave functions, corresponding to $u^s_l$ and $(u^s_l)^*$ at energy $E_i$. The constraints of Eq. (13) ensure that at the EST support points $E_i$ the exact and the separable Coulomb-distorted nuclear half-shell $t$ matrices are identical. For the explicit evaluation we insert a complete set of Coulomb states so that $g_c(E_{p_0})$ takes the form of a free Green's function. The generalization of the EST scheme to complex potentials of Ref. [15] is not affected by changing the basis from plane waves to Coulomb scattering states. Similar expressions for a Coulomb-distorted separable nuclear $t$ matrix are given in Refs. [10–12].

We write the separable Coulomb-distorted nuclear $t$-matrix elements as

$$\begin{aligned} \langle p' | \tau^{CN}_l(E_{p_0}) | p \rangle &\equiv \sum_{i,j} h^c_{l,i}(p') \tau^c_{ij}(E_{p_0}) h^c_{l,j}(p) \\ &= \sum_{i,j} \big\langle \Phi^c_{l,p'} \big| u^s_l \big| f^c_{l,k_{E_i}} \big\rangle \tau^c_{ij}(E_{p_0}) \\ &\quad \times \big\langle f^{c*}_{l,k_{E_j}} \big| u^s_l \big| \Phi^c_{l,p} \big\rangle, \end{aligned} \tag{14}$$

TABLE I. The partial-wave $S$-matrix elements for $j = l + 1/2$ as a function of selected angular momenta $l$ calculated for $p + {}^{48}Ca$ elastic scattering at laboratory kinetic energy $E_{lab} = 38$ MeV obtained from the CH89 [19] phenomenological optical potential. The second column gives the $S$-matrix element obtained with the separable representation of the momentum space calculation, which is given in the third column. In the last column the corresponding coordinate space calculations are given.

| $l$ | Separable | $p$ space | $r$ space |
|---|---|---|---|
| 0 | −0.0512 0.3765 | −0.0518 0.3768 | −0.0523 0.3767 |
| 2 | 0.3805 0.0420 | 0.3809 0.0421 | 0.3808 0.0427 |
| 6 | −0.0445 0.0170 | −0.0457 0.0118 | −0.0462 0.0111 |
| 10 | 0.9818 0.0248 | 0.9814 0.0253 | 0.9814 0.0253 |

where the form factor,

$$\begin{aligned} h^c_{l,i}(p) &\equiv \big\langle \Phi^c_{l,p} \big| u^s_l \big| f^c_{l,k_{E_i}} \big\rangle \\ &= \big\langle f^{c*}_{l,k_{E_i}} \big| u^s_l \big| \Phi^c_{l,p} \big\rangle = \langle p | \tau^{CN}_l(E_i) | k_{E_i} \rangle, \end{aligned} \tag{15}$$

is the short-ranged half-shell $t$ matrix satisfying Eq. (8). For our analysis, and the comparison with coordinate-space calculations, we consider the partial-wave $S$-matrix elements, which are obtained from the on-shell $t$-matrix elements by the relation $S_l(E_{p_0}) = 1 - 2\pi i \mu p_0 \langle p_0 | \tau^{CN}_l(E_{p_0}) | p_0 \rangle$.

Evaluating the separable Coulomb-distorted proton-nucleus $t$ matrix involves integrals over the proton-nucleus form factor $h^c_{l,i}(p)$. If the short-range Coulomb potential is omitted, the numerical integration is similar to the neutron-nucleus separable potentials discussed in Ref. [15]. However, if it is included, the proton-nucleus form factor falls off more slowly as a function of the momentum. This implies that for a finite momentum grid, one has to use a much larger value of the maximum momentum and a larger number of grid points to obtain a separable representation of the Coulomb-distorted proton-nucleus $t$ matrix with the same accuracy as the separable representation of the corresponding neutron-nucleus $t$ matrix.

For studying the quality of the separable representation of $t$ matrices for proton-nucleus optical potentials we consider elastic scattering of protons from $^{12}$C, $^{48}$Ca, and $^{208}$Pb in the range from 0 to 50 MeV laboratory kinetic energy. We use the CH89 global optical potential [19] and its rank-4 (rank-5) separable representations for $p + {}^{12}C$, $p + {}^{48}Ca$ ($p + {}^{208}Pb$). The same support points used for the neutron-nucleus separable representation (summarized in Table I of [15]) provide a description of equal quality for the proton-nucleus $S$-matrix elements. This is demonstrated for $p + {}^{48}Ca$ scattering at 38 MeV laboratory kinetic energy in Table I, which gives the $S$-matrix elements calculated with the separable representation of the Coulomb-distorted proton-nucleus $t$ matrix, together with the corresponding direct calculations performed either in momentum or coordinate space.

Similar results for the $p + {}^{208}Pb$ $S$-matrix elements are shown in Fig. 1. The top two panels (a) and (b) show the real and imaginary parts of the $S$-matrix elements for $j = l + 1/2$ at 10 MeV laboratory kinetic energy while the bottom two panels (c) and (d) show the real and imaginary

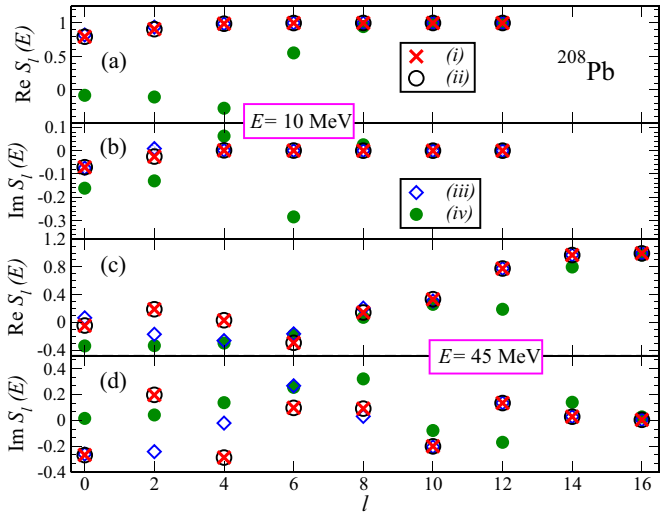


FIG. 1. (Color online) The partial-wave $S$ matrix for $p + {}^{208}Pb$ elastic scattering obtained from the CH89 [19] global optical potential as a function of the angular momentum. (a) and (b) show the real and imaginary parts of the $S$ matrix at 10 MeV laboratory kinetic energy; (c) and (d) give the real and imaginary parts of the $S$-matrix elements at 45 MeV laboratory kinetic energy. The total angular momentum is $j = l + 1/2$. The cross symbols (red) ($i$) give the $S$-matrix elements calculated from the momentum space separable representation of the CH89 global optical potential for $p + {}^{208}Pb$ elastic scattering, while open circles (black) ($ii$) depict the corresponding coordinate space calculation. The open diamonds (blue) ($iii$) show the calculation in which the short-range Coulomb potential is omitted. The solid circles (green) ($iv$) indicate the $S$-matrix elements for $n + {}^{208}Pb$ elastic scattering.

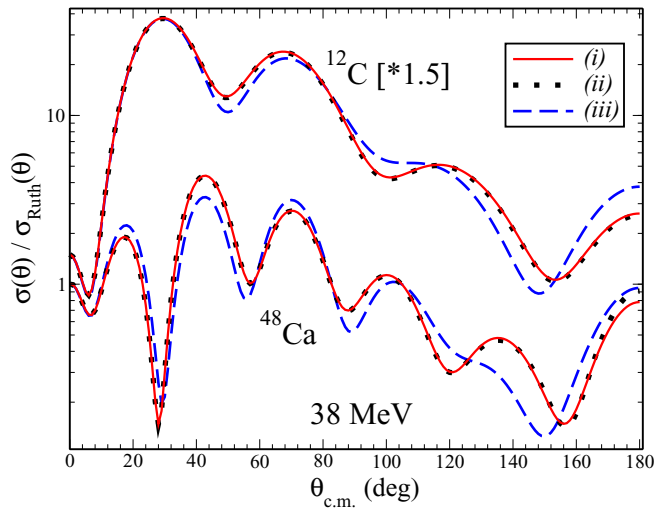


FIG. 2. (Color online) The unpolarized differential cross section for elastic scattering of protons from $^{12}$C (upper) and $^{48}$Ca (lower) divided by the Rutherford cross section as a function of the c.m. angle calculated for a laboratory kinetic energy of 38 MeV. The $^{12}$C cross section is scaled by a factor 1.5. The solid lines ($i$) depict the cross section calculated in momentum space based on the rank-4 separable representation of the CH89 [19] phenomenological optical potential, while the dotted lines ($ii$) represent the corresponding coordinate space calculations. The dashed lines ($iii$) show the results in which the short-ranged Coulomb potential is omitted.

parts of the $S$-matrix elements at 45 MeV. At 10 MeV the partial-wave series converges much faster, thus we do not show matrix elements beyond $l = 12$. First, we note that the momentum space $S$-matrix elements calculated with the separable representation (crosses) agree perfectly with the corresponding coordinate-space calculation (open circles). We find the same agreement for the $j = l - 1/2$ $S$-matrix elements.

To illustrate the effects of the short-range Coulomb potential on the $S$-matrix elements, we show a calculation in which this term is omitted (open diamonds). As indicated in Fig. 1, only the low $l$ partial waves are affected. To demonstrate the overall size of all Coulomb effects for $^{208}$Pb, we also plot the corresponding $n + {}^{208}Pb$ $S$-matrix elements at the same energies (solid circles). The differences between the crosses and the solid circles demonstrate the importance of the correct inclusion of the Coulomb interaction.

To further demonstrate the quality of the rank-4 separable representation of proton-nucleus optical potentials, we display in Fig. 2 the unpolarized differential cross sections divided by the Rutherford cross section for $p + {}^{12}C$ and $p + {}^{48}Ca$ at 38 MeV laboratory kinetic energy as a function of the c.m. angle. Here we also include the cross sections corresponding to the coordinate space solutions (dotted lines). As with the $S$ matrices in Fig. 1, there is excellent agreement between the momentum-space EST and the coordinate space results. Also shown are the calculations in which the short-range Coulomb potential of Eq. (2) is omitted (dashed lines). The differences between the solid and dashed lines demonstrate clearly the importance of including the short-range Coulomb term, even for light nuclei.

Next we examine the form factors of the separable representation in the Coulomb basis in detail. In Fig. 3 we compare $p + {}^{48}Ca$ form factors at the 36 MeV support point for selected angular momenta calculated with the proton-nucleus potential and the short-range Coulomb potential ($i$) to those calculated with the proton-nucleus potential alone ($ii$). We immediately observe that, with the exception of $l = 0$, the form factors already vanish at 3.5 fm$^{-1}$. For $l = 0$ we see that the short-range Coulomb potential significantly modifies the nuclear form factor. However, those effects quickly decrease as $l$ increases and almost vanish for $l = 6$ in $^{48}$Ca and $l = 8$ in $^{208}$Pb (not shown).

For further comparison we show in Fig. 3 the form factor of ($ii$) derived in a plane-wave basis ($iii$). For $l = 0$ this form factor has a finite value as $p \to 0$. To demonstrate the necessity of solving the integral equation, Eq. (8), as a starting point for the EST scheme, we include in Fig. 3 [dotted line ($iv$)], the plane-wave form factor $\langle \Phi^c_{l,p} | u^s_l | f_{l,k_{E_i}} \rangle$ (with $| f_{l,k_{E_i}} \rangle$ being the regular scattering wave function at energy $E_i$) evaluated in the Coulomb basis with the techniques introduced in [9]. This clearly indicates that the procedure outlined here is needed to obtain an accurate description of proton-nucleus scattering with a separable representation of the short-range force.

Summarizing, we have generalized the EST scheme [15,16] so that it can be applied to the scattering of charged

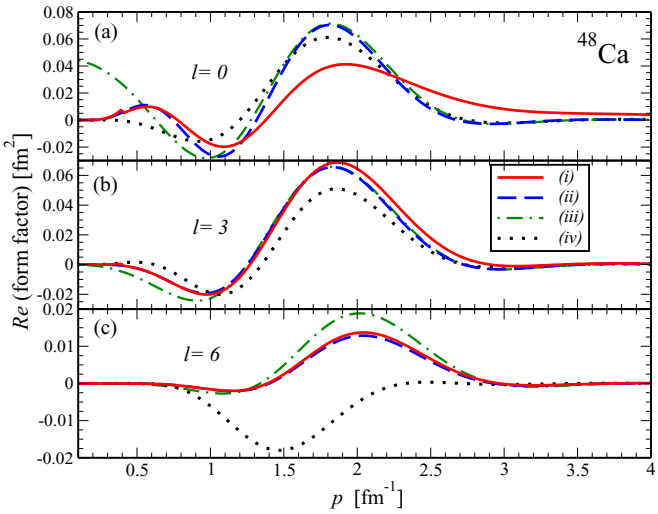


FIG. 3. (Color online) The real parts of the partial-wave proton-nucleus form factor for $^{48}$Ca as a function of the momentum $p$ for selected angular momenta $l$: (a) $l = 0$, (b) $l = 3$, and (c) $l = 6$. The form factors are calculated at $E_{\text{c.m.}} = 36$ MeV and based on the CH89 global optical potential: The full calculations ($i$) are compared to those omitting the short-range Coulomb ($ii$), the proton-nucleus form factor in the plane wave basis ($iii$), and the form factor obtained using the techniques introduced in [9] ($iv$).

particles with a repulsive Coulomb force. To demonstrate the feasibility and accuracy of our method, we applied this momentum-space Coulomb EST scheme to proton elastic scattering from $^{12}$C, $^{48}$Ca, and $^{208}$Pb. We found that the same EST support points employed to construct a separable representation of neutron-nucleus optical potentials can be used for the separable representation of the proton-nucleus potential. We showed that the momentum-space $S$-matrix elements calculated with the separable representation of the Coulomb-distorted proton-nucleus potential as well as the cross sections for elastic scattering agree very well with the corresponding coordinate-space calculation. Because changing from a plane wave to a Coulomb basis preserves the time-reversal invariance of the separable potential, the separable Coulomb-distorted proton-nucleus off-shell $t$ matrix also obeys reciprocity.

We also studied the effects of the short-range Coulomb potential on the proton-nucleus form factor. We found that, with the exception of the lowest partial waves the form factors already vanish at 3.5 fm$^{-1}$. For the lowest partial waves the short-range Coulomb force creates a very slow fall-off for the proton-nucleus form factor at high momenta. The effects of the short-range Coulomb potential quickly decrease as $l$ increases.

In addition, this work demonstrates that when using Coulomb-distorted form factors in A(d,p)B Faddeev reaction calculations carried out in a Coulomb-distorted partial-wave basis, it is mandatory to evaluate neutron and proton-nucleus form factors separately.

This material is based on work in part supported by the U.S. Department of Energy, Office of Science of Nuclear Physics under Programs No. DE-SC0004084 and No. DE-SC0004087 (TORUS Collaboration), under Contracts No. DE-FG52-08NA28552 with Michigan State University and No. DE-FG02-93ER40756 with Ohio University; and by Lawrence Livermore National Laboratory under Contract No. DE-AC52-07NA27344 and the U.T. Battelle LLC Contract No. DE-AC0500OR22725. F.M. Nunes acknowledges support from the National Science Foundation under Grant No. PHY-0800026. This research used resources of the National Energy Research Scientific Computing Center, which is supported by the Office of Science of the U.S. Department of Energy under Contract No. DE-AC02-05CH11231.

[1] R. Kozub, G. Arbanas, A. Adekola, D. Bardayan, J. Blackmon *et al.*, Phys. Rev. Lett. **109**, 172501 (2012).
[2] I. J. Thompson and F. M. Nunes, *Nuclear Reactions for Astrophysics* (Cambridge University Press, Cambridge, 2009).
[3] E. Alt, P. Grassberger, and W. Sandhas, Nucl. Phys. B **2**, 167 (1967).
[4] A. Deltuva and A. C. Fonseca, Phys. Rev. C **79**, 014606 (2009).
[5] A. Deltuva, A. C. Fonseca, and P. U. Sauer, Phys. Rev. C **71**, 054005 (2005).
[6] A. Deltuva, A. C. Fonseca, and P. U. Sauer, Phys. Rev. C **72**, 054004 (2005).
[7] F. Nunes and N. Upadhyay, J. Phys. G: Conf. Ser. **403**, 012029 (2012).
[8] A. M. Mukhamedzhanov, V. Eremenko, and A. I. Sattarov, Phys. Rev. C **86**, 034001 (2012).
[9] N. Upadhyay *et al.* (TORUS Collaboration), Phys. Rev. C **90**, 014615 (2014).
[10] S. K. Adhikari, Phys. Rev. C **14**, 782 (1976).
[11] W. Schweiger, W. Plessas, L. P. Kok, and H. van Haeringen, Phys. Rev. C **27**, 515 (1983).
[12] W. Schweiger, W. Plessas, L. P. Kok, and H. van Haeringen, Phys. Rev. C **28**, 1414 (1983).
[13] G. Cattapan, G. Pisent, and V. Vanzani, Z. Phys. A **274**, 139 (1975).
[14] G. Cattapan, G. Pisent, and V. Vanzani, Nucl. Phys. A **241**, 204 (1975).
[15] L. Hlophe *et al.* (TORUS Collaboration), Phys. Rev. C **88**, 064608 (2013).
[16] D. J. Ernst, C. M. Shakin, and R. M. Thaler, Phys. Rev. C **8**, 46 (1973).
[17] C. Elster, L. C. Liu, and R. M. Thaler, J. Phys. G **19**, 2123 (1993).
[18] C. R. Chinn, C. Elster, and R. M. Thaler, Phys. Rev. C **44**, 1569 (1991).
[19] R. Varner, W. Thompson, T. McAbee, E. Ludwig, and T. Clegg, Phys. Rep. **201**, 57 (1991).